Electronic Supplementary Material (ESI) for Physical Chemistry Chemical Physics.

ELECTRONIC SUPPORTING INFORMATION

Elucidation of factors shaping reactivity of 5'-deoxyadenosyl – a prominent organic radical in biology

Zuzanna Wojdyla,[a] Mauricio Maldonado-Domínguez,[a] Priyam Bharadwaz,[a] Martin Culka,[b]

and Martin Srnec[a,*]

[a] *J. Heyrovský Institute of Physical Chemistry, Czech Academy of Sciences, Dolejškova 3, 18200 Prague, Czech Republic*

[b] *Institute of Organic Chemistry and Biochemistry, Czech Academy of Sciences, Flemingovo nám. 2, 166 10 Prague, Czech Republic*

email address: martin.srnec@jh-inst.cas.cz

Table S1: The list of substrates (in different protonation states) native to radical SAM enzymes (also listed).

Number	Radical SAM enzyme	Substrates	Optimized structures of Substrates with highlighted HAA hydrogen	Total charge
1A	BioB	Dethiobiotin[1]	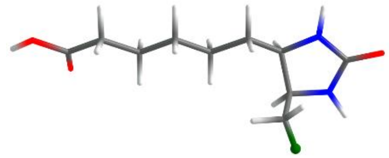	0
1B	BioB	Dethiobiotin[1]	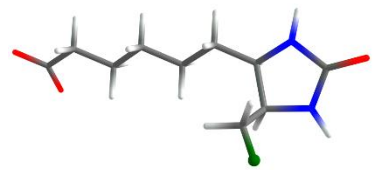	-1
2A	ThiC	5-aminoimidazole ribonucleotide[2]	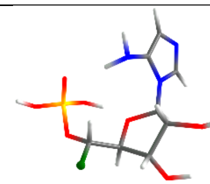	0
2B	ThiC	5-aminoimidazole ribonucleotide[2]	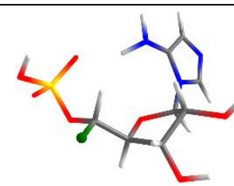	-1
2C	ThiC	5-aminoimidazole ribonucleotide[2]	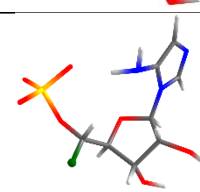	-2

3	LipA	Octanoyl derivative of the H-protein[3]	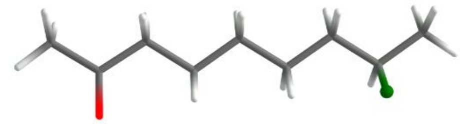	0
4	PFl-AE	PFL (Glycine residue)[4]	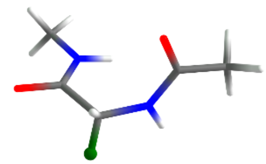	0
5	LAM	Lysine[5]	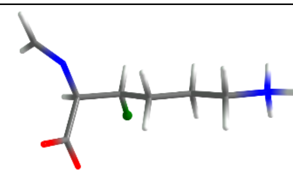	0
6A	EAM	Glutamic acid[6]	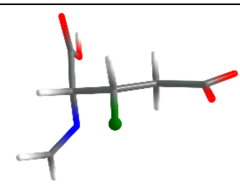	-1
6B	EAM	Glutamic acid[6]	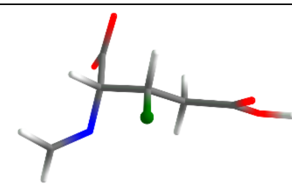	-1
6C	EAM	Glutamic acid[6]	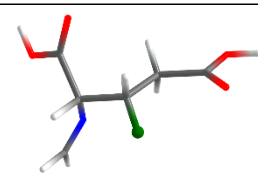	0

6D	EAM	Glutamic acid[6]	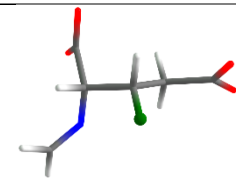	-2
7A	QueE	6-carboxy-5,6,7,8 tetrahydropterin[7]	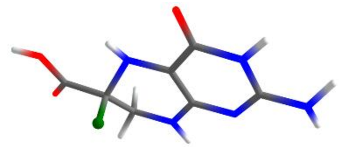	0
7B	QueE	6-carboxy-5,6,7,8-Tetrahydropterin[7]	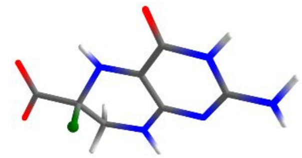	-1
8A	MqnC	Dehypoxanthine Futalosine[8]	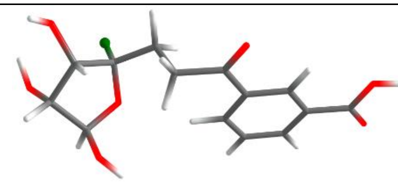	0
8B	MqnC	Dehypoxanthine Futalosine[8]	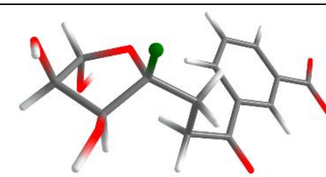	-1
9	SkfB	SkfB (cyclotriane)[9]	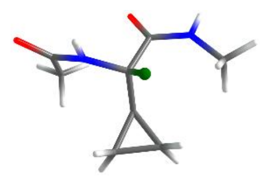	0

10A	NosL	CH_3-Tryptophan[10,11]	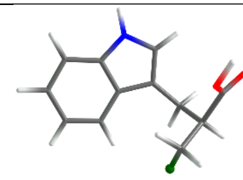	0
10B	NosL	CH_3-Tryptophan[10,11]	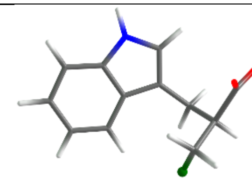	-1
11A	NosL	CH_2-Tryptophan[10,11]	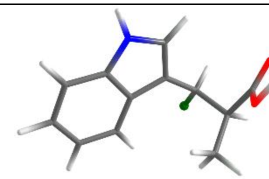	0
11B	NosL	CH_2-Tryptophan[10,11]	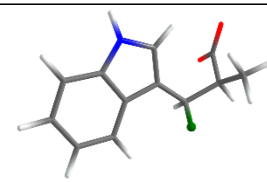	-1
12A	anSME	Thiol-based amino acid[12]	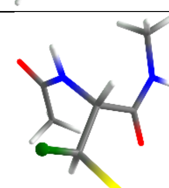	0
12B	anSME	Alcohol-based amino acid[12]	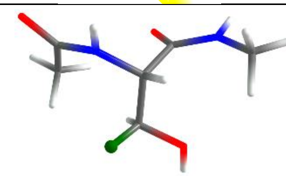	0

13A	BlsE	cytosylglucuronic acid (CGA), chair[13]	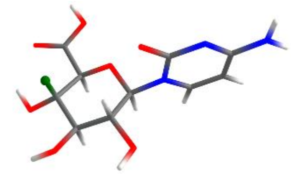	0
13B	BlsE	cytosylglucuronic acid (CGA), boat[13]	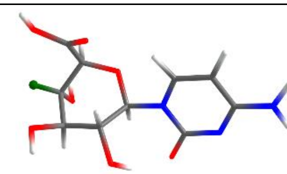	0
13C	BlsE	cytosylglucuronic acid (CGA), chair[13]	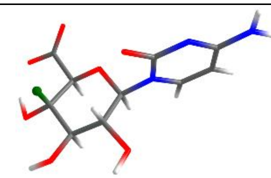	-1
13D	BlsE	cytosylglucuronic acid (CGA), boat[13]	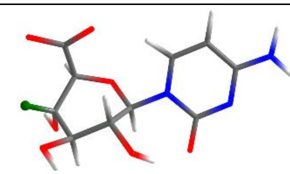	-1
14A	RimO	S12 aspartate 89[14]	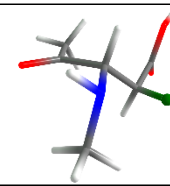	0
14B	RimO	S12 aspartate 89[14]	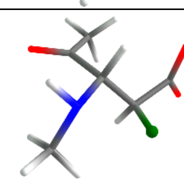	-1

15	MoaA	Guanosine 5′-triphosphate (GTP)[15]	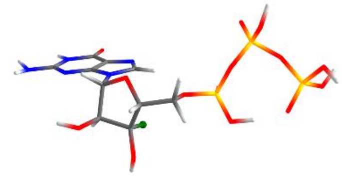	0
16	GenK	GenX2[16]	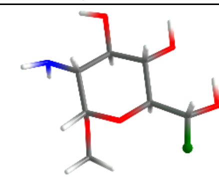	0
17A	DesII	TDP-ADG[17]	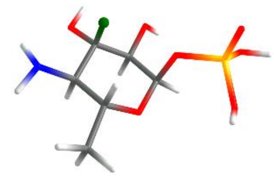	0
17B	DesII	TDP-ADG[17]	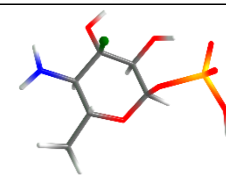	-1
17C	DesII	TDP-ADG[17]	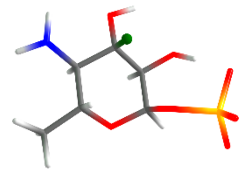	-2
18	OxsB	2′-deoxyadenosine-5′-monophosphate (dAMP)[18]	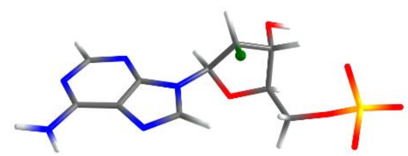	-2

19	RlmN/Cfr	Methyl- cysteinyl 355[19]	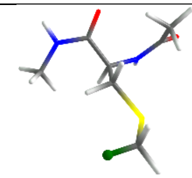	0
20	TYW1	N-methylguanosine[20]	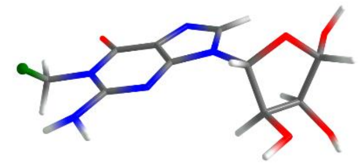	0
21A	Fom3	2-hydroxyethylphosphonate (HEP)[21]	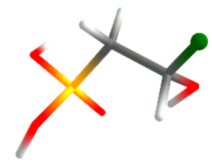	0
21B	Fom3	2-hydroxyethylphosphonate (HEP)[21]	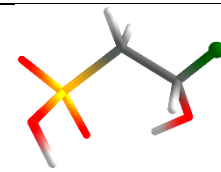	-1
21C	Fom3	2-hydroxyethylphosphonate (HEP)[21]	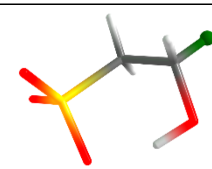	-2
22A	MftC	Tyrosine[22]	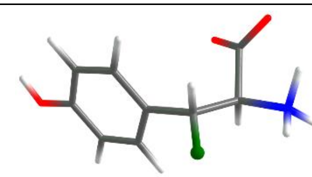	0

22B	MftC	Tyrosine[22]	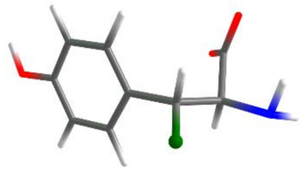	-1
22C	MftC	Tyrosine[22]	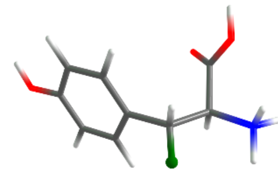	1
22D	MftC	Tyrosine[22]	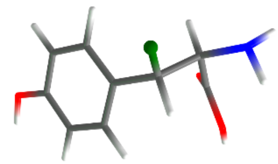	0
23A	PqqE	PqqE (Glu-cgamma)[23]	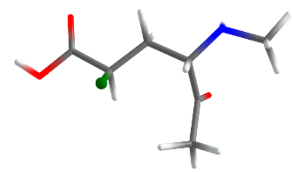	0
23B	PqqE	PqqE (Glu-cgamma)[23]	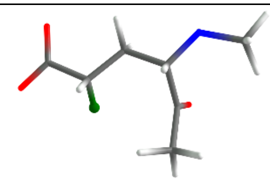	-1
24	PoyD	L-valine[24]	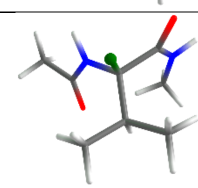	0

25	AprD4	Paromamine[25]	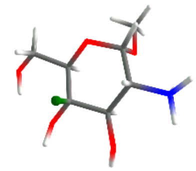	0
26	NosN	MTA[26]	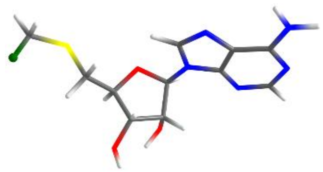	0
27	Alba	Alba[27]	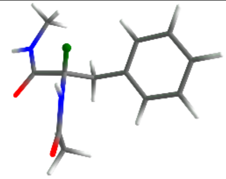	0
28	SkfB	Methionine[9]	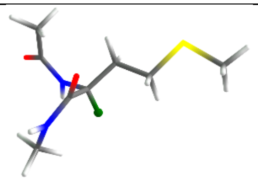	0

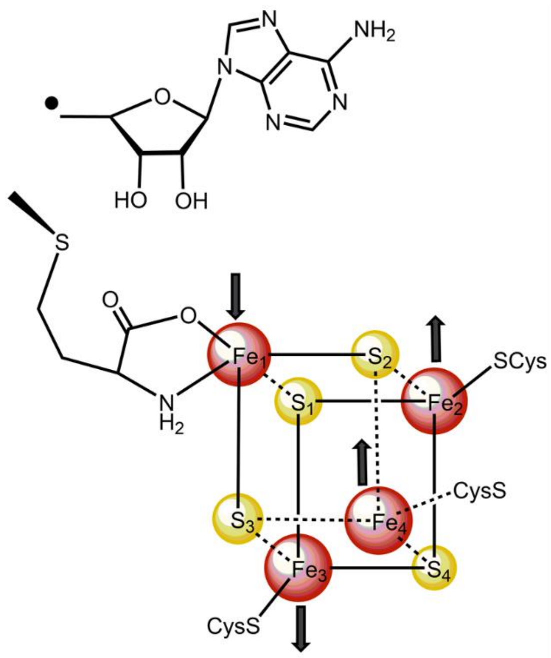

$[Fe_4S_4]^{2+}$ + dAdo$^{\bullet}$

	PFL-AE	LAM
	$[Fe_4S_4]^{2+}$ + dAdo$^{\bullet}$	$[Fe_4S_4]^{2+}$ + dAdo$^{\bullet}$
Fe_1	-3.649	-3.648
Fe_2	3.657	3.631
Fe_3	-3.743	-3.749
Fe_4	3.674	3.729
S_1	-0.137	-0.199
S_2	0.260	0.264
S_3	-0.134	-0.083
S_4	-0.137	0.068
C_5	1.014	1.025

Figure S1: Schematic representation of antiferromagnetic coupling present in PFL-AE and LAM with their corresponding Mulliken spin densities of key atoms.

Dihedral Dependence of Reactivity of the 5'dAdo$^{\bullet}$. The 5'dAdo$^{\bullet}$ radical is relatively flexible molecule. we selected HAA from the beta position of lysimine (representant of lysine), a reaction carried out by the lysine aminomutase (LAM) enzyme, as a model reaction. We explored all three routes along the entire torsional coordinate α of the adenyl-ribosyl C–N bond and the resulting reaction profiles are presented in **Figure 5**.

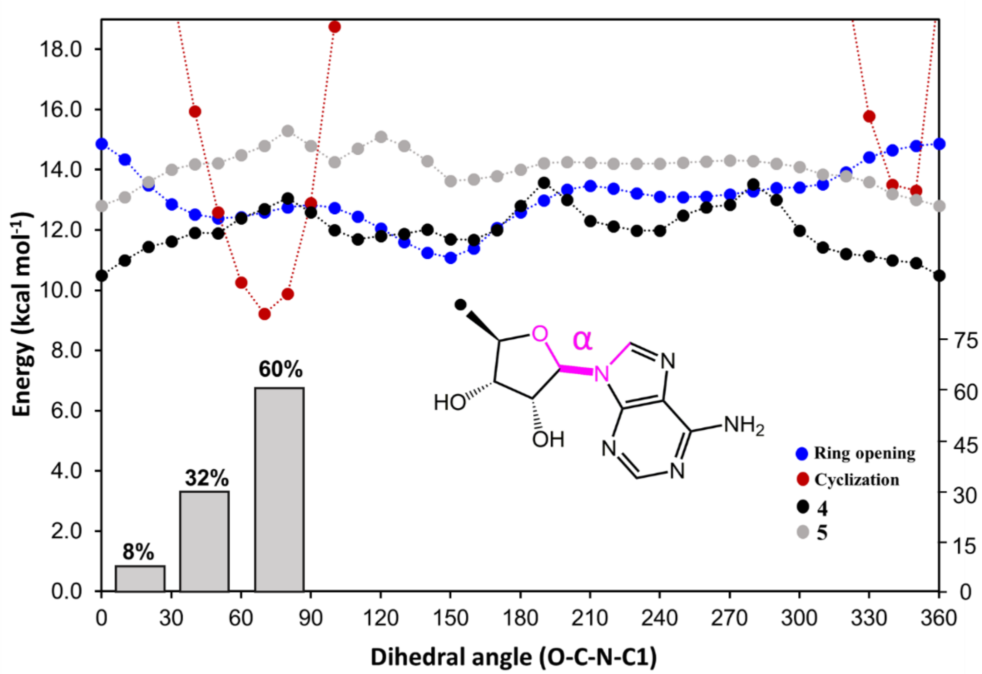

Figure S2. Potential energy barriers for the ring opening, cyclization and HAA reaction paths of the 5'dAdo• radical in homogeneous aqueous solution, as a function of the ribosyl-adenyl dihedral angle (shown in magenta). The histogram shows the population of different conformers in nature (determined by the dihedral angle as depicted in the figure), extracted from a snapshot of the PDB database (see the table below). The RC-to-TS HAA reaction involves the abstraction of H-atom from the beta position in lysimine. For each point, the reactant complex (RC) and the corresponding transition state (TS) were optimized with constraints on a given dihedral angle.

Table S2: The dihedral angle within the SAM or SAH, which defines the position of the adenine relative to the ribose ring – Y[O4'-C1'-N9-C8]

PDB ID	resolution (Å)	(residue name)_(residue id)_(chain id)	dihedral angle O4'-C1'-N9-C8 (deg)
2a5h	2.1	SAM_417_A	69.4
2a5h	2.1	SAM_417_B	65.9

2a5h	2.1	SAM_417_C	63.5
2a5h	2.1	SAM_417_D	62.8
1r30	3.4	SAM_501_A	26.7
1r30	3.4	SAM_501_B	32.4
1olt	2.07	SAM_501_A	43.2
2fb2	2.25	SAM_501_A	40.9
2fb2	2.25	SAM_501_B	42.7
4r34	1.8	SAH_503_A	78.7
4r34	1.8	SAH_503_B	80.4
3rfa	2.05	SAM_406_A	76.2
3rfa	2.05	SAM_406_B	65.8
5wgg	2.04	SAM_504_A	71.2
3cix	1.7	SAH_1501_A	56.2
4jye	1.65	SAH_402_A	54
5fep	1.45	SAM_407_A	53.6
5vsl	1.97	SAH_402_A	81.7
5vsl	1.97	SAH_402_B	85.5
3ciw	1.35	SAH_1501_A	57
3cb8	2.77	SAM_501_A	62.8
5fes	1.27	SAM_408_A	54.2
4njh	1.9	SAM_302_A	69
4njh	1.9	SAM_302_B	71
3iiz	1.62	SAM_1501_A	49.5

5ff2	1.47	SAH_408_A	56.7
5ff3	1.18	SAH_410_A	66.7
3t7v	1.5	SAM_992_A	41.9
4k37	1.62	SAM_504_A	85.1
4k37	1.62	SAM_504_B	89.5
2a5h	2.1	SAM_417_A	69.4
2a5h	2.1	SAM_417_B	65.9
2a5h	2.1	SAM_417_C	63.5
2a5h	2.1	SAM_417_D	62.8
1r30	3.4	SAM_501_A	26.7
1r30	3.4	SAM_501_B	32.4
1olt	2.07	SAM_501_A	43.2
6htk	2	SAH_508_A	76.1
6htk	2	SAH_502_B	79.4
6q2p	1.45	SAH_402_A	78.1
6q2p	1.45	SAH_403_B	80.8
2fb2	2.25	SAM_501_A	40.9
2fb2	2.25	SAM_501_B	42.7
6bxo	1.66	SAH_901_A	13.3
6bxo	1.66	SAH_901_B	19.1
6fz6	1.42	SAH_402_A	78.8
6fz6	1.42	SAH_402_B	75.3
6efn	1.29	SAM_501_A	77.2

6q2q	1.89	SAH_402_A	78.9
6q2q	1.89	SAH_402_B	82.2

Comment on Dihedral Dependence of Reactivity of the 5'dAdo•. The 5'dAdo• radical is relatively flexible molecule. we selected HAA from the beta position of lysimine (representant of lysine), a reaction carried out by the lysine aminomutase (LAM) enzyme, as a model reaction. We explored all three routes along the entire torsional coordinate α of the adenyl-ribosyl C–N bond and the resulting reaction profiles are presented in **Figure S1**. To better understand **Figure S1**, let first focus on the histogram at the bottom-left corner. It shows a narrow range of conformations, mostly within the 60-90°, for adenyl-ribosyl torsion that SAM occupies in structurally characterized radical SAM enzymes (**Table associated with Figure S1**). Since the initial reductive cleavage of SAM into methionine and 5'dAdo• is unlikely to change this torsion angle, we conclude that the 5'dAdo• keeps this narrow torsional window while abstracting hydrogen atom from a wide range of natural substrates. Now, we observe that the undesired cyclization (CYC) and ring-opening decay (ROD) routes for 5'dAdo• show conformation-dependent reaction barrier profiles (in red and and blue in **Figure S1**), and that the barrier for both is accessible within this narrow torsional window. The final and most striking observation is that the favored conformational range lies precisely in the domain where HAA is the least accessible process of all. This single example highlights that 5'dAdo•-containing enzymes must have evolved to guarantee their metabolic proficiency by favoring a costly process while simultaneously disfavoring two very competitive unwanted side reactions.

Table S3: Free energies of all substrates and their oxidized, deprotonated and dehydrogenated conjugates, all together forming half-reaction thermodynamic cycles along with the key half-reaction thermodynamic properties, as depicted in **Scheme 4**. Two off-diagonal themodynamic factors (η' and σ' - see the equations in the main text) associated with the reaction of the substrate with the methyl radical. The blue highlighted lines indicate species, for which the half-reaction off-diagonal thermodynamic properties are inaccessible due to the instability of the oxidized and/or deprotonated conjugate of the AH species. For these species, the η' and σ' were obtained employing the calibration lines from **Figure 6** in the main text.

Subst.	G_{A-H} (au)	$G_{A-H^{\cdot+}}$ (au)	G_{A^-} (au)	$G_{A^\cdot}$ (au)	$(RT/F)\ln 10$ $pK_{a,AH}$ (mV)	$(RT/F)\ln 10$ $pK_{a,A^\cdot}$ (mV)	E°_{AH} (mV)	$E^\circ_{A^\cdot}$ (mV)	η' (mV)	σ' (mV)
1A	-727,241716	-727,004272	-726,688835	-726,584547	3511	-109	2181	-1442	1922	-1864
1B	-726,782138	-726,577009	-726,229176	-726,126680	3513	723	1302	-1491	2544	-2418
2A	-1345,866283	-1345,676379	-	-1345,212363	-	-	-	-	1341	-2090
2B	-1345,425120	-1345,244703	-	-1344,778612	-	-	-	-	2313	-1835
2C	-1344,948090	-	-	-1344,307529	-	-	-	-	3035	-1646
3	-484,400052	-484,14888	-483,827204	-483,750066	4054	-678	2555	-2181	2042	-940
4	-456,641906	-456,391488	-456,12886	-456,001921	2428	-929	2534	-826	906	-1720
5	-535,180756	-534,965715	-534,613003	-534,529912	3915	328	1572	-2019	2638	-1765
6A	-589,418483	-589,210585	-588,85792	-588,766181	3720	562	1377	-1784	2637	-2097
6B	-589,425053	-589,210664	-588,860766	-588,773336	3821	369	1554	-1901	2584	-1878
6C	-589,875855	-589,630162	-589,328978	-589,223152	3348	-455	2406	-1400	1647	-1649
6D	-588,964250	-588,760754	-588,385362	-588,311994	4218	680	1257	-2284	3075	-1827
7A	-771,855779	-771,685957	-771,356969	-771,247420	2041	402	341	-1299	2182	-2327
7B	-771,405695	-771,250929	-770,854407	-770,783421	3467	1190	-69	-2348	3481	-2142
8A	-1069,948519	-1069,689838	-1069,401735	-1069,308628	3345	-1156	2759	-1746	1396	-909
8B	-1069,496615	-1069,282688	-1068,946286	-1068,856390	3441	70	1541	-1834	2325	-1714
9	-972,762990	-972,537685	-972,264725	-972,130414	2026	-448	1851	-625	1104	-2202
10A	-670,443099	-670,242837	-669,883323	-669,785617	3698	910	1169	-1621	2769	-2458

10B	-669,985024	-669,797472	-669,40747	-669,329376	4181	1206	824	-2155	3355	-2290
11A	-670,443099	-670,24284	-669,901474	-669,808166	3205	297	1169	-1741	2420	-1940
11B	-669,983578	-669,790495	-669,42661	-669,352163	3622	397	974	-2254	2853	-1648
12A	-894,155892	-893,924928	-893,631427	-893,512954	2738	-320	2005	-1056	1500	-1988
12B	-571,176637	-570,932453	-570,627427	-570,535147	3411	-719	2365	-1769	1722	-1202
13A	-1080,031227	-1079,792117	-1079,492002	-1079,383738	3140	-418	2227	-1334	1627	-1723
13B	-1080,026310	-1079,791009	-1079,496838	-1079,386351	2874	-519	2123	-1273	1513	-1694
13C	-1079,588831	-	-1079,031741	-1078,945807	-	-	-	-	2667	-1742
13D	-1079,580517	-	-1079,032899	-1078,942906	-	-	-	-	1992	-1919
14A	-515,79764	-515,589376	-515,30602	-515,155083	1845	287	1387	-173	1304	-3042
14B	-515,344869	-	-514,80753	-514,700463	-	-	-	-	2024	-1911
15	-2742,720036	-2742,508517	-	-2742,077613	-	-	-	-	1810	-1967
16	-706,757144	-706,528665	-706,19786	-706,110260	3685	-145	1937	-1896	2217	-1518
17A	-1160,106434	-1159,877227	-1159,558704	-1159,459630	3371	-167	1957	-1584	1981	-1723
17B	-1159,670880	-1159,447136	-1159,11618	-1159,021162	3560	61	1808	-1694	2220	-1806
17C	-1159,193514	-1159,007542	-1158,626863	-1158,543155	3885	1105	781	-2002	3176	-2327
18	-1455,495986	-1455,316621	-1454,954704	-1454,840884	3195	1414	601	-1183	2815	-3124
19	-933,455907	-933,224711	-932,919626	-932,810726	3059	-265	2011	-1317	1722	-1843
20	-1039,049308	-1038,841039	-1038,517326	-1038,398924	2943	500	1387	-1058	2080	-2566
21A	-722,934997	-	-722,380179	-722,290040	-	-	-	-	2138	-1881
21B	-722,494297	-722,258646	-721,924407	-721,851339	3973	-447	2132	-2292	2284	-1025
21C	-722,012937	-721,83451	-721,427179	-721,372732	4405	1034	575	-2798	3689	-1714
22A	-630,153928	-629,938968	-	-629,521975	-	-	-	-	1818	-1965
22B	-629,701211	-	-629,161444	-629,067571	-	-	-	-	2424	-1806
22C	-630,584311	-630,355225	-	-629,951037	-	-	-	-	1292	-2103
22D	-630,156547	-629,936176	-629,628494	-629,520584	2836	-221	1717	-1344	1772	-1854
23A	-555,108983	-554,89837	-554,610202	-554,466237	2040	228	1451	-362	1397	-2866
23B	-554,651992	-554,451049	-554,103312	-554,007930	3397	527	1188	-1685	2543	-2143
24	-574,540862	-574,29670	-574,032564	-573,911419	2299	-1045	2364	-983	935	-1526
25	-707,190411	-706,92947	-706,654836	-706,541845	3040	-982	2821	-1205	1137	-1415

26	-1326,048574	-1325,824093	-1325,509848	-1325,403981	3126	-99	1828	-1399	1899	-1902
27	-727,001719	-726,758711	-726,50146	-726,371342	2080	-989	2333	-739	803	-1739
28	-573,313651	-573,061033	-572,81281	-572,686886	2096	-1348	2594	-853	629	-1404
$5'dAdo^{\cdot}$	-888,524515	-	-	-887,866057	-	-	-	-	2060	-1902
$CH_3^{\cdot}$	-40,510798	-40,16991	-39,954431	-39,848654	3606	-2786	4996	-1402	0	0

Table S4: The AIM charge of H-atom in the substrate ($q_{\mathrm{H}}(\mathrm{substrate})$) as well as in the TS of the reaction between AH (substrate or 5'dAdoH) and the methyl radical ($q_{\mathrm{H}}(\mathrm{substrate})|_{\mathrm{TS}}$); $\Delta q_{\mathrm{H}}(\mathrm{substrate})|_{\mathrm{polarization}}$ – charge polarization on H-atom, *i.e.*, the change of the charge on H along the R-to-TS trajectory but in the absence of the methyl radical at the TS (single point calculation of the substrate geometry at the TS); $\Delta q_{\mathrm{H}}|_{\mathrm{R-to-TS}}$ – the change of charge of H-atom in going from separated reactants to TS; charge polarization corrected $\Delta q_{\mathrm{H}}|_{\mathrm{R-to-TS}}$ – the difference of the 4th and 3rd column; $\Delta q_{\mathrm{CH}_3^{\cdot}}|_{\mathrm{R-to-TS}}$ – the change of charge on the methyl radical going from separated reactants to TS; the $\Delta Q'$ and $\Delta Q''$ are the charge redistribution descriptors defined in the main text.

Substrates	$q_{\mathrm{H}}(\mathrm{substrate})$ (e)	$q_{\mathrm{H}}(\mathrm{substrate})\|_{\mathrm{TS}}$ (e)	$\Delta q_{\mathrm{H}}(\mathrm{substrate})\|_{\mathrm{polarization}}$ (e)	$\Delta q_{\mathrm{H}}\|_{\mathrm{R-to-TS}}$ (e)	**Polarization-corrected $\Delta q_{\mathrm{H}}\|_{\mathrm{R-to-TS}}$ (e)**	**$\Delta q_{\mathrm{CH}_3^{\cdot}}\|_{\mathrm{R-to-TS}}$ (e)**	**$\Delta Q'$ (e)**	**$\Delta Q''$ (e)**
1A	0,012	-0,002	-0,014	0,128	0,142	-0,068	0,1049	0,0056
1B	0,011	-0,003	-0,014	0,129	0,143	-0,069	0,1056	0,0063
2A	0,069	0,060	-0,009	0,084	0,093	-0,034	0,0634	-0,0359
2B	0,027	0,002	-0,026	0,115	0,140	-0,083	0,1119	0,0127
2C	-0,007	-0,042	-0,034	0,137	0,172	-0,124	0,1479	0,0487
3	-0,019	-0,041	-0,022	0,15004	0,172	-0,10114	0,1366	0,0373
4	0,063	0,063	0,000	0,087	0,087	-0,031	0,0590	-0,0402
5	0,009	-0,013	-0,022	0,1323	0,154	-0,0879	0,1211	0,0218
6A	0,012	-0,009	-0,020	0,1265	0,147	-0,0774	0,1122	0,0129
6B	0,019	-0,013	-0,032	0,1179	0,150	-0,0815	0,1158	0,0166
6C	0,033	0,018	-0,015	0,11058	0,126	-0,057	0,0915	-0,0078
6D	0,008	-0,031	-0,039	0,1295	0,169	-0,1025	0,1355	0,0363
7A	0,042	0,036	-0,006	0,085	0,091	-0,054	0,0725	-0,0268
7B	-0,008	-0,027	-0,020	0,124	0,143	-0,122	0,1327	0,0334
8A	0,031	0,009	-0,021	0,111	0,132	-0,078	0,1050	0,0058
8B	0,029	0,007	-0,022	0,112	0,134	-0,081	0,1071	0,0079
9	0,053	0,060	0,007	0,084	0,077	-0,010	0,0435	-0,0557

10A	0,011	-0,006	-0,017	0,131	0,148	-0,077	0,1126	0,0133
10B	-0,010	-0,036	-0,026	0,150	0,176	-0,105	0,1407	0,0414
11A	0,022	0,004	-0,018	0,114	0,132	-0,084	0,1081	0,0089
11B	0,007	-0,011	-0,018	0,129	0,147	-0,102	0,1246	0,0254
12A	0,057	0,045	-0,012	0,097	0,109	-0,065	0,0869	-0,0124
12B	0,027	0,004	-0,023	0,113	0,136	-0,080	0,1083	0,0091
13A	0,035	0,008	-0,027	0,105	0,132	-0,072	0,1021	0,0028
13B	0,062	0,052	-0,010	0,092	0,103	-0,053	0,0777	-0,0216
13C	0,006	-0,024	-0,030	0,127	0,157	-0,102	0,1296	0,0303
13D	0,055	0,037	-0,019	0,099	0,118	-0,074	0,0959	-0,0034
14A	0,071	0,084	0,013	0,080	0,067	0,005	0,0357	-0,0635
14B	0,018	0,015	-0,003	0,124	0,127	-0,068	0,0975	-0,0018
15	0,042	0,026	-0,016	0,097	0,113	-0,060	0,0867	-0,0125
16	0,031	-0,004	-0,034	0,112	0,146	-0,090	0,1179	0,0186
17A	0,028	0,006	-0,022	0,115	0,137	-0,081	0,1091	0,0099
17B	0,0183	-0,010	-0,029	0,121	0,150	-0,098	0,1243	0,0250
17C	0,0139	-0,018	-0,032	0,127	0,159	-0,108	0,1334	0,0341
18	0,024	0,030	0,006	0,116	0,111	-0,047	0,0789	-0,0204
19	0,043	0,027	-0,016	0,112	0,128	-0,080	0,1039	0,0047
20	0,042	0,027	-0,015	0,100	0,115	-0,048	0,0813	-0,0179
21A	0,036	0,010	-0,026	0,107	0,133	-0,073	0,1031	0,0039
21B	0,009	-0,025	-0,034	0,126	0,160	-0,107	0,1335	0,0343
21C	-0,021	-0,062	-0,041	0,145	0,186	-0,142	0,1639	0,0647
22A	0,023	0,014	-0,009	0,107	0,116	-0,058	0,0871	-0,0121
22B	0,002	-0,008	-0,011	0,133	0,144	-0,091	0,1174	0,0182
22C	0,049	0,043	-0,005	0,088	0,093	-0,029	0,0609	-0,0383
22D	0,019	0,007	-0,011	0,118	0,130	-0,065	0,0973	-0,0019
23A	0,049	0,058	0,009	0,089	0,080	-0,002	0,0413	-0,0580
23B	-0,004	-0,012	-0,008	0,135	0,143	-0,077	0,1099	0,0107
24	0,049	0,049	0,000	0,090	0,090	-0,029	0,0599	-0,0393

25	0,041	0,013	-0,027	0,098	0,125	-0,064	0,0943	-0,0049
26	0,040	0,024	-0,016	0,115	0,131	-0,084	0,1074	0,0082
27	0,049	0,056	0,008	0,086	0,078	-0,017	0,0476	-0,0517
28	0,049	0,058	0,008	0,088	0,080	-0,018	0,0487	-0,0505
5′dAdoH	0,012	0,010	-0,001	0,134	0,135	-0,064	0,0992	-

Table S5: The AIM charge of H-atom in the substrate ($q_{\mathrm{H}}(\mathrm{substrate})$) as well as in the TS of the reaction between substrate and the 5'-deoxyadenosyl radical ($q_{\mathrm{H}}(\mathrm{substrate})|_{\mathrm{TS}}$); $\Delta q_{\mathrm{H}}(\mathrm{substrate})|_{\mathrm{polarization}}$ – charge polarization on H-atom, *i.e.*, the change of the charge on H along the R-to-TS trajectory but in the absence of the 5'-deoxyadenosyl at the TS (single point calculation of the substrate geometry at the TS); $\Delta q_{\mathrm{H}}|_{\mathrm{R-to-TS}}$ – the change of charge of H-atom in going from separated reactants to TS; charge polarization corrected $\Delta q_{\mathrm{H}}|_{\mathrm{R-to-TS}}$ – the difference of the 4th and 3rd column; $\Delta q_{5'\mathrm{dAdo}^{\cdot}}|_{\mathrm{R-to-TS}}$ – the change of charge on the 5'-deoxyadenosyl radical going from separated reactants to TS; the ΔQ^{*} and ΔQ^{**} are the charge redistribution descriptors defined in the main text.

Substrates	$q_{\mathrm{H}}(\mathrm{substrate})$ (e)	$q_{\mathrm{H}}(\mathrm{substrate})\|_{\mathrm{TS}}$ (e)	$\Delta q_{\mathrm{H}}(\mathrm{substrate})\|_{\mathrm{polarization}}$ (e)	$\Delta q_{\mathrm{H}}\|_{\mathrm{R-to-TS}}$ (e)	**Polarization-corrected $\Delta q_{\mathrm{H}}\|_{\mathrm{R-to-TS}}$ (e)**	**$\Delta q_{5'\mathrm{dAdo}^{\cdot}}\|_{\mathrm{R-to-TS}}$ (e)**	**ΔQ^{*} (e)**	**ΔQ^{**} (e)**
1A	0,012	-0,005	-0,017	0,130	0,147	-0,079	0,1130	0,0086
1B	0,011	-0,006	-0,017	0,130	0,148	-0,079	0,1135	0,0090
2A	0,069	0,056	-0,013	0,084	0,097	-0,047	0,0720	-0,0325
2B	0,027	-0,004	-0,031	0,117	0,148	-0,104	0,1259	0,0214
2C	-0,007	-0,049	-0,042	0,142	0,184	-0,151	0,1672	0,0628
3	-0,019	-0,046	-0,027	0,153	0,180	-0,103	0,1415	0,0371
4	0,063	0,052	-0,011	0,092	0,103	-0,059	0,0811	-0,0233
5	0,009	-0,015	-0,024	0,134	0,158	-0,107	0,1324	0,0280
6A	0,012	-0,007	-0,019	0,131	0,150	-0,071	0,1102	0,0058
6B	0,019	-0,016	-0,035	0,121	0,156	-0,102	0,1288	0,0244
6C	0,033	0,014	-0,019	0,109	0,128	-0,074	0,1009	-0,0036
6D	0,008	-0,035	-0,043	0,133	0,176	-0,141	0,1584	0,0539
7A	0,042	0,030	-0,012	0,092	0,103	-0,088	0,0957	-0,0087
7B	-0,008	-0,036	-0,028	0,134	0,162	-0,160	0,1609	0,0564
8A	0,031	0,001	-0,030	0,110	0,140	-0,105	0,1226	0,0181
8B	0,029	-0,001	-0,030	0,112	0,142	-0,111	0,1263	0,0219
9	0,053	0,057	0,004	0,087	0,082	-0,015	0,0486	-0,0559

10A	0,011	-0,010	-0,021	0,134	0,154	-0,091	0,1226	0,0181
10B	-0,010	-0,039	-0,028	0,152	0,180	-0,131	0,1553	0,0509
11A	0,022	0,006	-0,016	0,119	0,135	-0,104	0,1195	0,0150
11B	0,007	-0,017	-0,024	0,132	0,155	-0,141	0,1483	0,0438
12A	0,057	0,037	-0,020	0,098	0,118	-0,086	0,1020	-0,0025
12B	0,027	-0,002	-0,030	0,114	0,143	-0,095	0,1194	0,0149
13A	0,035	-0,010	-0,045	0,101	0,146	-0,074	0,1097	0,0053
13B	0,062	0,049	-0,013	0,078	0,092	-0,064	0,0777	-0,0267
13C	0,006	-0,032	-0,038	0,130	0,168	-0,122	0,1451	0,0406
13D	0,055	0,030	-0,025	0,104	0,129	-0,103	0,1161	0,0116
14A	0,071	0,081	0,010	0,080	0,070	-0,008	0,0392	-0,0652
14B	0,018	0,013	-0,005	0,128	0,133	-0,102	0,1175	0,0130
15	0,042	0,016	-0,026	0,106	0,132	-0,093	0,1126	0,0081
16	0,031	-0,012	-0,042	0,115	0,158	-0,113	0,1354	0,0309
17A	0,028	0,000	-0,028	0,115	0,143	-0,104	0,1237	0,0193
17B	0,0183	-0,005	-0,023	0,129	0,152	-0,115	0,1334	0,0290
17C	0,0139	-0,010	-0,024	0,136	0,160	-0,124	0,1420	0,0376
18	0,024	0,025	0,000	0,118	0,118	-0,081	0,0996	-0,0049
19	0,043	0,022	-0,020	0,115	0,135	-0,097	0,1159	0,0114
20	0,042	0,023	-0,019	0,104	0,123	-0,049	0,0856	-0,0188
21A	0,036	0,001	-0,034	0,109	0,143	-0,110	0,1267	0,0222
21B	0,009	-0,035	-0,044	0,130	0,174	-0,137	0,1554	0,0509
21C	-0,021	-0,070	-0,049	0,148	0,197	-0,164	0,1805	0,0761
22A	0,023	0,013	-0,010	0,112	0,122	-0,046	0,0839	-0,0205
22B	0,002	-0,016	-0,018	0,135	0,153	-0,110	0,1311	0,0267
22C	0,049	0,044	-0,004	0,090	0,095	0,017	0,0558	-0,0487
22D	0,019	0,005	-0,013	0,120	0,133	-0,083	0,1082	0,0037
23A	0,049	0,061	0,011	0,094	0,082	-0,002	0,0418	-0,0626
23B	-0,004	-0,014	-0,010	0,139	0,149	-0,076	0,1125	0,0081
24	0,049	0,045	-0,004	0,090	0,095	-0,029	0,0618	-0,0427

25	0,041	0,016	-0,025	0,096	0,120	-0,054	0,0872	-0,0172
26	0,040	0,019	-0,021	0,117	0,138	-0,111	0,1246	0,0202
27	0,049	0,050	0,001	0,086	0,084	-0,025	0,0546	-0,0499
28	0,049	0,052	0,003	0,088	0,085	-0,028	0,0563	-0,0481

Table S6: The key off-diagonal thermodynamic characteristics for the HAA reactions of substrates with the 5'-deoxyadenosyl radical.

Reaction: $5'dAdo^{·}$ + Substrates	σ (mV)	η (mV)	$\Delta E^{\circ} = \frac{1}{\sqrt{2}}(\sigma + \eta)$ (mV)	$(RT/F)\ln 10\ \Delta pK_{a,A^{·}} = \frac{1}{\sqrt{2}}(\sigma - \eta)$ (mV)	$\frac{1}{4}(\lvert\sigma\rvert - \lvert\eta\rvert) = \Delta G^{\neq}_{offdiag}$ (kcal mol^{-1})
1A	-37,6	138,3	71,2	-124,3	-0,6
1B	516,2	-484,5	22,4	707,6	0,2
2A	188,2	718,7	641,3	-375,1	-3,1
2B	-66,9	-253,4	-226,4	131,9	-1,1
2C	-256,2	-975,0	-870,6	508,3	-4,1
3	-962,0	17,8	-667,6	-692,8	5,4
4	-181,5	1153,8	687,6	-944,2	-5,6
5	-136,4	-578,7	-505,6	312,7	-2,5
6A	195,4	-577,6	-270,3	546,6	-2,2
6B	-23,6	-524,5	-387,5	354,2	-2,9
6C	-252,4	412,3	113,1	-470,0	-0,9
6D	-74,4	-1014,8	-770,2	665,0	-5,4
7A	425,3	-122,1	214,4	387,1	1,7
7B	240,2	-1421,0	-835,0	1174,6	-6,8
8A	-993,1	663,5	-233,0	-1171,4	1,9
8B	-188,1	-265,0	-320,4	54,3	-0,4
9	300,7	955,4	888,2	-462,9	-3,8
10A	556,5	-709,1	-107,9	895,0	-0,9
10B	388,2	-1295,6	-641,6	1190,6	-5,2
11A	38,5	-360,4	-227,6	282,0	-1,9
11B	-254,1	-793,6	-740,8	381,5	-3,1
12A	86,4	560,2	457,2	-335,1	-2,7
12B	-699,6	338,2	-255,6	-733,8	2,1
13A	-179,2	432,9	179,4	-432,8	-1,5

13B	-207,9	547,2	239,9	-533,9	-2,0
13C	-159,7	-607,1	-542,2	316,4	-2,6
13D	17,4	67,6	60,1	-35,5	-0,3
14A	1140,1	755,8	1340,6	271,7	2,2
14B	9,0	35,7	31,6	-18,9	-0,2
15	65,3	250,2	223,1	-130,8	-1,1
16	-384,1	-157,5	-382,9	-160,2	1,3
17A	-178,8	78,9	-70,7	-182,2	0,6
17B	-95,8	-160,2	-181,0	45,5	-0,4
17C	425,0	-1116,2	-488,8	1089,8	-4,0
18	1222,5	-755,0	330,6	1398,4	2,7
19	-59,2	337,4	196,7	-280,4	-1,6
20	664,4	-20,5	455,3	484,3	3,7
21A	-20,9	-78,1	-69,9	40,4	-0,3
21B	-877,0	-223,7	-778,3	-461,9	3,8
21C	-188,2	-1629,1	-1285,0	1018,9	-8,3
22A	63,2	242,2	215,9	-126,6	-1,0
22B	-96,1	-364,7	-325,8	189,9	-1,5
22C	201,1	767,8	685,1	-400,7	-3,3
22D	-47,3	287,4	169,8	-236,7	-1,4
23A	964,4	663,2	1150,9	213,0	1,7
23B	240,8	-482,8	-171,1	511,6	-1,4
24	-375,3	1124,7	529,9	-1060,7	-4,3
25	-487,2	922,8	308,0	-997,0	-2,5
26	0,2	161,2	114,2	-113,8	-0,9
27	-162,5	1257,3	774,1	-1003,9	-6,3
28	-497,4	1430,7	660,0	-1363,4	-5,4

Table S7: Energetics of the HAA reactions of substrates with the 5'-deoxyadenosyl radical: free energies of separated reactants, separated products, reactant complexes (RC) and product complexes (PC), free energies of formation of RC and PC, the free energy of reaction in going from separated reactants to separated products as well as the free energy of reaction in going from RC to PC.

Substrates	$G_{\mathrm{A-H}}$ (au)	$G_{\mathrm{A^{\bullet}}}$ (au)	G_{RC} (au)	G_{TS} (au)	G_{PC} (au)	w_{R} (kcal mol^{-1})	w_{P} (kcal mol^{-1})	$\Delta G_{0,\mathrm{inf}}$ (kcal mol^{-1})	ΔG_0 (kcal mol^{-1})
1A	-727,241716	-726,584547	-1615,102289	-1615,07224	-1615,107969	1,5	-1,2	-0,8	-3,6
1B	-726,782138	-726,126680	-1614,640354	-1614,611336	-1614,647614	3,0	0,3	-1,9	-4,6
2A	-1345,866283	-1345,212363	-2233,72678	-2233,700594	-2233,731977	1,6	1,2	-2,8	-3,3
2B	-1345,425120	-1344,778612	-2233,283188	-2233,263866	-2233,296494	3,1	2,3	-7,5	-8,3
2C	-1344,948090	-1344,307529	-2232,805574	-2232,789297	-2232,822895	3,5	3,8	-11,2	-10,9
3	-484,400052	-483,750066	-1372,258855	-1372,236261	-1372,267719	2,7	2,4	-5,3	-5,6
4	-456,641906	-456,001921	-1344,488977	-1344,470505	-1344,507733	10,0	9,8	-11,6	-11,8
5	-535,180756	-534,529912	-1423,034405	-1423,012618	-1423,039191	5,9	7,7	-4,8	-3,0
6A	-589,418483	-588,766181	-1477,277073	-1477,254172	-1477,284418	2,8	2,0	-3,9	-4,6
6B	-589,425053	-588,773336	-1477,276038	-1477,25757	-1477,285193	7,6	6,0	-4,2	-5,7
6C	-589,875855	-589,223152	-1477,730261	-1477,708813	-1477,738028	5,4	4,1	-3,6	-4,9
6D	-588,964250	-588,311994	-1476,816445	-1476,795815	-1476,824231	6,8	5,8	-3,9	-4,9
7A	-771,855779	-771,247420	-1659,718224	-1659,709848	-1659,767953	0,4	0,6	-31,4	-31,2
7B	-771,405695	-770,783421	-1659,266811	-1659,25677	-1659,303143	1,2	1,1	-22,7	-22,8
8A	-1069,948519	-1069,308628	-1957,812229	-1957,791351	-1957,833103	-0,4	-1,9	-11,7	-13,1
8B	-1069,496615	-1068,856390	-1957,355857	-1957,338495	-1957,376448	2,4	0,9	-11,4	-12,9
9	-972,762990	-972,130414	-1860,623963	-1860,602025	-1860,647509	1,3	2,8	-16,2	-14,8
10A	-670,443099	-669,785617	-1558,305099	-1558,274514	-1558,309823	0,6	-1,7	-0,6	-3,0
10B	-669,985024	-669,329376	-1557,845117	-1557,815884	-1557,84967	1,8	0,7	-1,8	-2,9
11A	-670,443099	-669,808166	-1558,30783	-1558,282821	-1558,330327	-1,1	-0,4	-14,8	-14,1
11B	-669,983578	-669,352163	-1557,844267	-1557,82528	-1557,866343	1,5	4,6	-17,0	-13,9
12A	-894,155892	-893,512954	-1782,01745	-1781,994069	-1782,030903	0,9	2,2	-9,7	-8,4
12B	-571,176637	-570,535147	-1459,037145	-1459,01587	-1459,053932	1,6	1,7	-10,6	-10,5

13A	-1080,031227	-1079,383738	-1967,894206	-1967,87483	-1967,905332	0,0	-0,1	-6,9	-7,0
13B	-1080,026310	-1079,386351	-1967,887872	-1967,866582	-1967,910026	0,9	-1,4	-11,6	-13,9
13C	-1079,588831	-1078,945807	-1967,446619	-1967,430627	-1967,459894	3,3	4,6	-9,7	-8,3
13D	-1079,580517	-1078,942906	-1967,442405	-1967,41579	-1967,458659	0,7	3,6	-13,1	-10,2
14A	-515,79764	-515,155083	-1403,65575	-1403,638947	-1403,671901	3,1	2,9	-10,0	-10,1
14B	-515,344869	-514,700463	-1403,203144	-1403,182577	-1403,216572	3,0	3,4	-8,8	-8,4
15	-2742,720036	-2742,077613	-3630,584984	-3630,56273	-3630,595577	-1,2	2,2	-10,1	-6,6
16	-706,757144	-706,110260	-1594,613379	-1594,592807	-1594,624169	4,3	4,8	-7,3	-6,8
17A	-1160,106434	-1159,459630	-2047,966362	-2047,943972	-2047,983763	1,9	-1,7	-7,3	-10,9
17B	-1159,670880	-1159,021162	-2047,525748	-2047,506459	-2047,537634	5,1	3,1	-5,5	-7,5
17C	-1159,193514	-1158,543155	-2047,044223	-2047,026166	-2047,05617	7,7	5,3	-5,1	-7,5
18	-1455,495986	-1454,840884	-2343,35596	-2343,330349	-2343,363707	1,9	-0,8	-2,1	-4,9
19	-933,455907	-932,810726	-1821,315023	-1821,293126	-1821,32603	2,5	3,9	-8,3	-6,9
20	-1039,049308	-1038,398924	-1926,908908	-1926,886022	-1926,919307	2,2	0,7	-5,1	-6,5
21A	-722,934997	-722,290040	-1610,792547	-1610,768673	-1610,803034	3,4	5,3	-8,5	-6,6
21B	-722,494297	-721,851339	-1610,349972	-1610,3286	-1610,365423	4,6	4,6	-9,7	-9,7
21C	-722,012937	-721,372732	-1609,876135	-1609,851684	-1609,893492	-0,1	0,5	-11,5	-10,9
22A	-630,153928	-629,521975	-1518,019064	-1517,998845	-1518,044813	-1,3	-0,8	-16,6	-16,2
22B	-629,701211	-629,067571	-1517,558565	-1517,53948	-1517,585442	3,6	2,3	-15,6	-16,9
22C	-630,584311	-629,951037	-1518,449007	-1518,432273	-1518,474593	-1,0	-1,3	-15,8	-16,1
22D	-630,156547	-629,520584	-1518,013697	-1517,993204	-1518,036245	3,7	3,7	-14,1	-14,1
23A	-555,108983	-554,466237	-1442,969198	-1442,948563	-1442,984691	1,8	1,9	-9,9	-9,7
23B	-554,651992	-554,007930	-1442,510501	-1442,491932	-1442,523026	2,8	4,0	-9,0	-7,9
24	-574,540862	-573,911419	-1462,401991	-1462,381252	-1462,431638	1,2	0,8	-18,2	-18,6
25	-707,190411	-706,541845	-1595,053365	-1595,03141	-1595,062787	0,0	0,3	-6,2	-5,9
26	-1326,048574	-1325,403981	-2213,906221	-2213,882316	-2213,921201	3,4	2,7	-8,7	-9,4
27	-727,001719	-726,371342	-1614,863037	-1614,841397	-1614,889588	1,1	2,0	-17,6	-16,7
28	-573,313651	-572,686886	-1461,172623	-1461,156028	-1461,201239	2,5	4,5	-19,9	-18,0
5′dAdo(H)	-888,524515	-887,866057		-		-	-	-	-

Table S8: Energetics of the HAA reactions of substrates with the 5'-deoxyadenosyl radical: the total HAA barrier for the reaction between a substrate and 5'dAdo• in going from separated reactants to TS (non-tunneling regime); the RC-to-TS part of the HAA barrier (non-tunneling regime); the diagonal thermodynamic contribution to the barrier; the off-diagonal thermodynamic contribution to the barrier; the three-component thermodynamic contribution to the barrier; the intrinsic barrier in the non-tunneling regime (all contributions besides the diagonal one); the $\Delta G^{\neq}_{00}$ - the intrinsic barrier without the off-diagonal thermodynamic contribution (non-tunneling regime); the tunneling contribution to the barrier. See eq 8 in the main text.

Reaction: 5′dAdo˙ + Substrates	$\Delta G^{\neq}_{\mathrm{HAA,total}}$ (kcal mol^{-1})	$\Delta G^{\neq}_{\mathrm{HAA}}$ (kcal mol^{-1})	$\Delta G^{\neq}_{\mathrm{diag}}$ (kcal mol^{-1})	$\Delta G^{\neq}_{\mathrm{offdiag}} = \frac{1}{4}(\lvert\sigma\rvert - \lvert\eta\rvert)$ (kcal mol^{-1})	$\Delta G^{\neq}_{\mathrm{thermo}}$ (kcal mol^{-1})	$\Delta G^{\neq}_{\mathrm{intrinsic}}$ (kcal mol^{-1})	$\Delta G^{\neq}_{00}$ (kcal mol^{-1})	$\Delta G^{\neq}_{\mathrm{tun}}$ $-RTln(\kappa)$ (kcal mol^{-1})
1A	20,4	18,9	-1,8	-0,6	-2,4	20,6	21,2	-2,48
1B	21,2	18,2	-2,3	0,2	-2,1	20,5	20,3	-2,45
2A	18,0	16,4	-1,6	-3,1	-4,7	18,1	21,1	-2,25
2B	15,2	12,1	-4,2	-1,1	-5,2	16,3	17,4	-1,85
2C	13,7	10,2	-5,4	-4,1	-9,6	15,6	19,8	-1,26
3	16,8	14,2	-2,8	5,4	2,7	17,0	11,5	-1,99
4	21,6	11,6	-5,9	-5,6	-11,5	17,5	23,1	-1,62
5	19,6	13,7	-1,5	-2,5	-4,1	15,2	17,7	-1,98
6A	17,2	14,4	-2,3	-2,2	-4,5	16,7	18,9	-1,89
6B	19,1	11,6	-2,9	-2,9	-5,8	14,5	17,3	-1,73
6C	18,9	13,5	-2,4	-0,9	-3,4	15,9	16,8	-1,92
6D	19,7	12,9	-2,4	-5,4	-7,9	15,4	20,8	-1,83
7A	5,6	5,3	-15,6	1,7	-13,9	20,9	19,1	-0,38
7B	7,5	6,3	-11,4	-6,8	-18,2	17,7	24,5	-0,41
8A	12,7	13,1	-6,5	1,9	-4,6	19,7	17,8	-2,35
8B	13,3	10,9	-6,5	-0,4	-6,9	17,4	17,8	-1,70

9	15,1	13,8	-7,4	-3,8	-11,2	21,2	24,9	-2,05
10A	19,8	19,2	-1,5	-0,9	-2,4	20,7	21,6	-2,35
10B	20,2	18,3	-1,4	-5,2	-6,7	19,8	25,0	-2,25
11A	14,6	15,7	-7,1	-1,9	-8,9	22,8	24,6	-2,08
11B	13,4	11,9	-6,9	-3,1	-10,0	18,8	22,0	-1,49
12A	15,6	14,7	-4,2	-2,7	-7,0	18,9	21,6	-2,31
12B	14,9	13,4	-5,3	2,1	-3,2	18,6	16,5	-2,10
13A	12,2	12,2	-3,5	-1,5	-5,0	15,6	17,1	-1,98
13B	14,3	13,4	-7,0	-2,0	-8,9	20,3	22,3	-2,07
13C	13,3	10,0	-4,2	-2,6	-6,7	14,2	16,8	-1,53
13D	17,4	16,7	-5,1	-0,3	-5,4	21,8	22,1	-2,36
14A	13,6	10,5	-5,1	2,2	-2,9	15,6	13,4	-1,42
14B	15,9	12,9	-4,2	-0,2	-4,4	17,1	17,3	-1,79
15	12,8	14,0	-3,3	-1,1	-4,4	17,3	18,4	-2,29
16	17,2	12,9	-3,4	1,3	-2,1	16,3	15,0	-1,78
17A	16,0	14,0	-5,5	0,6	-4,9	19,5	18,9	-1,99
17B	17,2	12,1	-3,7	-0,4	-4,1	15,8	16,2	-1,73
17C	19,1	11,3	-3,7	-4,0	-7,7	15,1	19,1	-1,67
18	18,0	16,1	-2,4	2,7	0,3	18,5	15,8	-2,51
19	16,2	13,7	-3,5	-1,6	-5,1	17,2	18,8	-2,29
20	16,5	14,4	-3,3	3,7	0,4	17,6	13,9	-2,00
21A	18,4	15,0	-3,3	-0,3	-3,6	18,3	18,6	-2,01
21B	18,0	13,4	-4,8	3,8	-1,1	18,3	14,5	-1,68
21C	15,2	15,3	-5,4	-8,3	-13,8	20,8	29,1	-1,30
22A	11,4	12,7	-8,1	-1,0	-9,1	20,8	21,8	-1,71
22B	15,5	12,0	-8,4	-1,5	-10,0	20,4	22,0	-1,72
22C	9,5	10,5	-8,0	-3,3	-11,3	18,5	21,8	-1,71
22D	16,5	12,9	-7,1	-1,4	-8,5	19,9	21,3	-1,91
23A	14,7	12,9	-4,9	1,7	-3,1	17,8	16,1	-1,69
23B	14,5	11,7	-3,9	-1,4	-5,3	15,6	17,0	-1,62

24	14,2	13,0	-9,3	-4,3	-13,6	22,3	26,6	-1,97
25	13,8	13,8	-3,0	-2,5	-5,5	16,7	19,2	-1,90
26	18,4	15,0	-4,7	-0,9	-5,6	19,7	20,6	-2,29
27	14,7	13,6	-8,3	-6,3	-14,6	21,9	28,2	-2,37
28	13,0	10,4	-9,0	-5,4	-14,4	19,4	24,8	-1,81

Table S9. Free energies of substrates and their oxidized, deprotonated and dehydrogenated conjugates, all together forming half-reaction thermodynamic cycles along with the key half-reaction thermodynamic properties, as depicted in **Scheme 4**, calculated with M06 functional. Two off-diagonal thermodynamic factors (η' and σ' - see the equations in the main text) associated with the reaction of the substrate with the methyl radical.

Subst.	$G_{\mathrm{A-H}}$ (au)	$G_{\mathrm{A-H^{\bullet+}}}$ (au)	$G_{\mathrm{A^-}}$ (au)	$G_{A^\bullet}$ (au)	$\left(\frac{RT}{F}\right)\ln 10\, pK_{\mathrm{a,AH}}$ (mV)	$\left(\frac{RT}{F}\right)\ln 10\, pK_{\mathrm{a,A}}$ (mV)	E°_{AH} (mV)	E°_{A} (mV)	η' (mV)	σ' (mV)
1A	-726.73722	-726.493415	-726.186194	-726.082069	3460	-337	2354	-1447	1767	-1732
4	-456.333168	-456.079726	-455.822657	-455.691873	2359	-976	2617	-721	803	-1793
5	-534.797119	--	-534.233608	-534.145891	3800	---	---	-1893	---	---
6C	-589.513097	-589.266699	-588.970471	-588.862057	3232	-519	2425	-1330	1556	-1685
7A	-771.372853	-771.200659	-770.873075	-770.763976	2067	352	406	-1311	2158	-2314
7B	-770.922147	-770.765109	-770.371605	-770.300596	3447	1108	-7	-2348	3426	-2116
11A	-669.953535	-669.751476	-669.408275	-669.315966	3304	320	1218	-1768	2459	-1969
12B	-570.800932	-570.551141	-570.254903	-570.16531	3325	-1031	2517	-1842	1556	-961

13D	-1078.931267	-1078.76032	-1078.383448	-1078.297692	3373	1057	372	-1946	3106	-2364
15	-2741.695807	-2741.48019	-2741.155562	-2741.053796	3167	72	1587	-1511	-1119	-1017
16	-706.313878	-706.080193	-705.755454	-705.668459	3661	-326	2079	-1913	2104	-1409
17C	-1158.702009	-1158.506944	-1158.137738	-1158.056696	3820	721	1028	-2075	2959	-2035
21C	-721.770847	-721.587962	-721.185524	-721.131558	4393	888	697	-2811	3598	-1633
22A	-629.721297	-629.505764	-629.204359	-629.08942	2534	-201	1585	-1152	1655	-2036
26	-1325.39439	-1325.162103	-1324.859179	-1324.750233	3030	-323	2041	-1315	1684	-1834
$CH_3^{\bullet}$	-40.468304	-40.126484	-39.911188	-39.806139	3511	-109	2181	-1442		

Table S10: Energetics of the HAA reactions of substrates with the 5'-deoxyadenosyl radical calculated with M06 functional: free energies of separated reactants, separated products, reactant complexes (RC) and product complexes (PC), free energies of formation of RC and PC, the free energy of reaction in going from separated reactants to separated products as well as the free energy of reaction in going from RC to PC.

Substrates	G_{A-H} (au)	$G_{A^{\bullet}}$ (au)	G_{RC} (au)	G_{TS} (au)	G_{PC} (au)	w_R (kcal mol^{-1})	w_P (kcal mol^{-1})	$\Delta G_{0,inf}$ (kcal mol^{-1})	ΔG_0 (kcal mol^{-1})
1A	-726.73722	-726.082069	-1614.012234	-1613.982649	-1614.018491	4.3	2.3	-1.9	-3.9
4	-456.333168	-455.691873	-1343.596956	-1343.578016	-1343.615475	11.3	10.3	-10.6	-11.6
5	-534.797119	-534.145891	-1422.072951	-1422.047759	-1422.081911	3.8	2.5	-4.4	-5.6
6C	-589.513097	-588.862057	-1476.788135	-1476.762274	-1476.797273	4.3	3.0	-4.5	-5.7
7A	-771.372853	-770.763976	-1658.654544	-1658.642044	-1658.701605	0.1	1.5	-31.0	-29.5
7B	-770.922147	-770.300596	-1658.202079	-1658.191387	-1658.236445	1.2	2.6	-23.0	-21.6
11A	-669.953535	-669.315966	-1557.229194	-1557.208024	-1557.259112	3.9	-1.9	-13.0	-18.8
12B	-570.800932	-570.16531	-1458.081026	-1458.055431	-1458.101836	1.1	2.2	-14.2	-13.1
13D	-1078.931267	-1078.297692	-1966.210588	-1966.183413	-1966.230213	1.6	4.7	-15.5	-12.3

15	-2741.695807	-2741.053796	-3628.980247	-3628.95338	-3628.992515	-1.6	0.8	-10.2	-7.7
16	-706.313878	-705.668459	-1593.589517	-1593.566467	-1593.59942	3.9	5.7	-8.0	-6.2
17C	-1158.702009	-1158.056696	-2045.96568	-2045.943201	-2045.976266	11.4	12.9	-8.1	-6.6
21C	-721.770847	-721.131558	-1609.049579	-1609.025789	-1609.070393	1.9	0.8	-11.9	-13.1
22A	-629.721297	-629.08942	-1517.001168	-1516.983373	-1517.030634	1.2	-0.7	-16.5	-18.5
26	-1325.39439	-1324.750233	-2212.671204	-2212.645428	-2212.681814	3.1	5.3	-8.8	-6.7
5′dAdo·	-887.940052	-887.281825							

Table S11. Energetics of the HAA reactions of substrates with the 5'-deoxyadenosyl radical calculated with M06 functional: the total HAA barrier for the reaction between a substrate and 5'dAdo• in going from separated reactants to TS (non-tunneling regime); the RC-to-TS part of the HAA barrier (non-tunneling regime); the diagonal thermodynamic contribution to the barrier; the off-diagonal thermodynamic contribution to the barrier; the three-component thermodynamic contribution to the barrier; the intrinsic barrier in the non-tunneling regime (all contributions besides the diagonal one); the $\Delta G^{\neq}_{00}$ - the intrinsic barrier without the off-diagonal thermodynamic contribution (non-tunneling regime);

Reaction: $5'dAdo^{\bullet}$ + Substrates	$\Delta G^{\neq}_{\mathrm{HAA,total}}$ (kcal mol^{-1})	$\Delta G^{\neq}_{\mathrm{HAA}}$ (kcal mol^{-1})	$\Delta G^{\neq}_{\mathrm{diag}}$ (kcal mol^{-1})	$\Delta G^{\neq}_{\mathrm{offdiag}}$ (kcal mol^{-1})	$\Delta G^{\neq}_{\mathrm{thermo}}$ (kcal mol^{-1})	$\Delta G^{\neq}_{\mathrm{intrinsic}}$ (kcal mol^{-1})	$\Delta G^{\neq}_{00}$ (kcal mol^{-1})
1A	22.8	18.6	-2.0	-0.7	-2.7	20.5	21.2
4	23.2	11.9	-5.8	-6.6	-12.4	17.7	24.3
5	19.6	15.8	-2.8	-2.9	-5.7	18.6	21.6
6C	20.5	16.2	-2.9	-1.7	-4.5	19.1	20.8
7A	7.9	7.8	-14.8	1.8	-13.0	22.6	20.8
7B	7.9	6.7	-10.8	-6.6	-17.4	17.5	24.1
11A	17.2	13.3	-9.4	-1.9	-11.3	22.7	24.6
12B	17.1	16.1	-6.5	2.5	-4.0	22.6	20.1

13D	18.6	17.1	-6.2	---	---	23.2	---
15	15.2	16.9	-3.8	---	---	20.7	---
16	18.3	14.5	-3.1	2.6	-0.5	17.6	15.0
17C	25.5	14.1	-3.3	-4.4	-7.7	17.4	21.8
21C	16.9	14.9	-6.5	---	---	21.5	---
22A	12.4	11.2	-9.2	-7.3	-16.6	20.4	27.7
26	19.3	16.2	-3.3	-1.6	-4.9	19.5	21.1

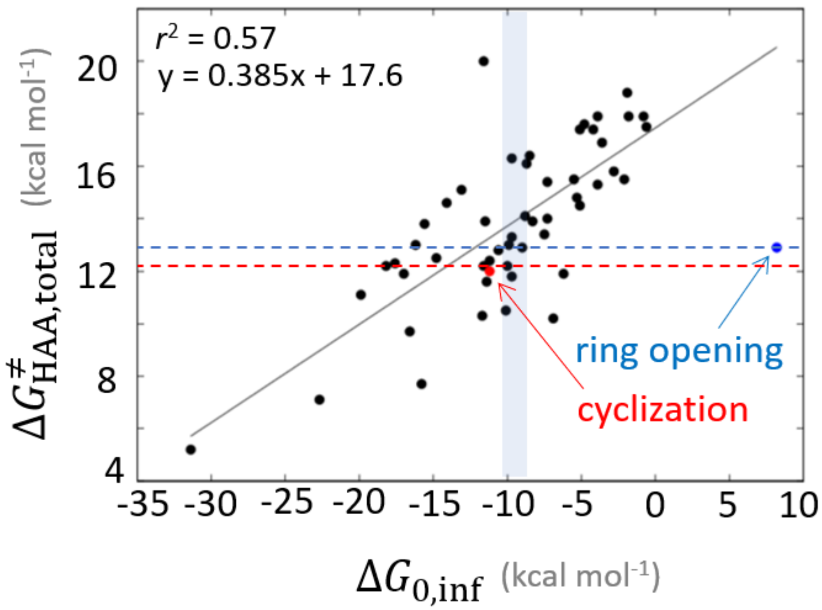

Figure S3. Correlation plot between the tunneling-corrected bimolecular free-energy barrier $\Delta G^{\neq}_{\mathrm{HAA,total}}$ and the free energy of HAA reaction $\Delta G_{0,\mathrm{inf}}$, known as linear free-energy relationship. The grey zone exemplifies points that do not follow LFER.

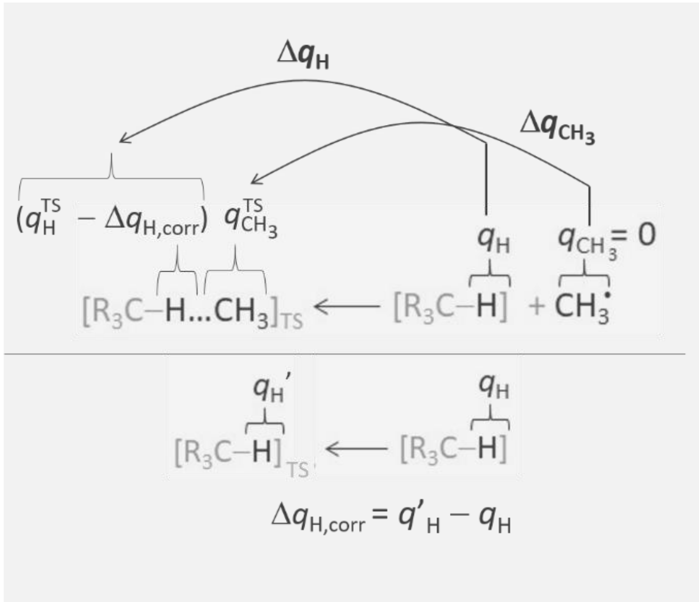

Figure S4. The description of the change of charge on the transferred hydrogen and the methyl radical in going from separated reactants to transition state in reactions between substrates/5'-deoxyadenosine and the methyl radical. The charge polarization on H-atom is also depicted. This polarization serves as a correction to the change of charge on H-atom along the reaction coordinate. The analogous approach was adopted for the evaluation of the change of charges in the reaction between substrates and 5'-deoxyadenosyl radical.

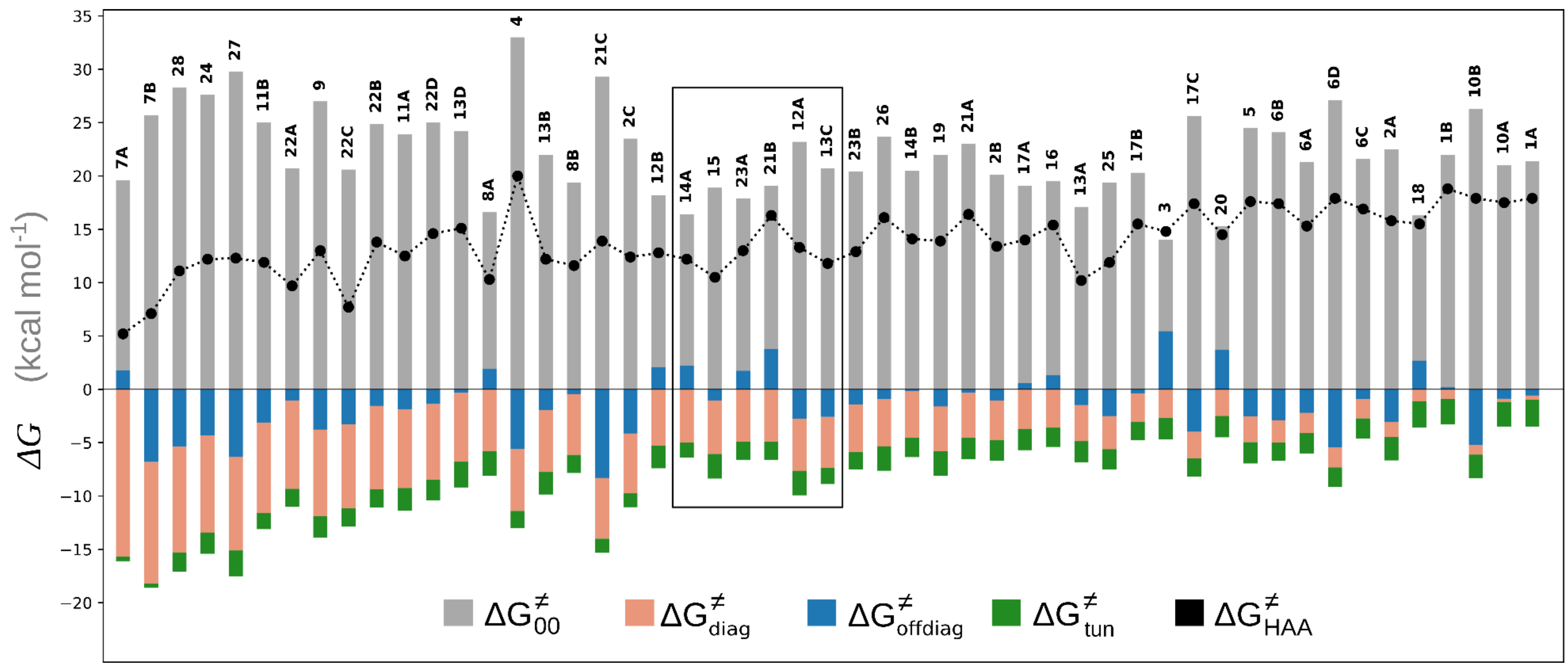

Figure S5. The free energy barrier $\Delta G^{\neq}$ for bimolecular (total) HAA reactions between 5'dAdo$^{\bullet}$ and C–H bond substrates from **Figure 2** of the main text (in black), calculated in aqueous solution. The total (bimolecular) barrier $\Delta G^{\neq}_{\mathrm{HAA,total}}$ was decomposed into four terms (following the eq 8 from the main text). Bimolecular HAA reactions are indicated by the labels used for the substrates in **Figure 2**. The reactions are ordered following the decrease in the magnitude of the diagonal contribution to the barrier. The reactions in a black frame correspond to the vertical grey zone in **Figure S4**.

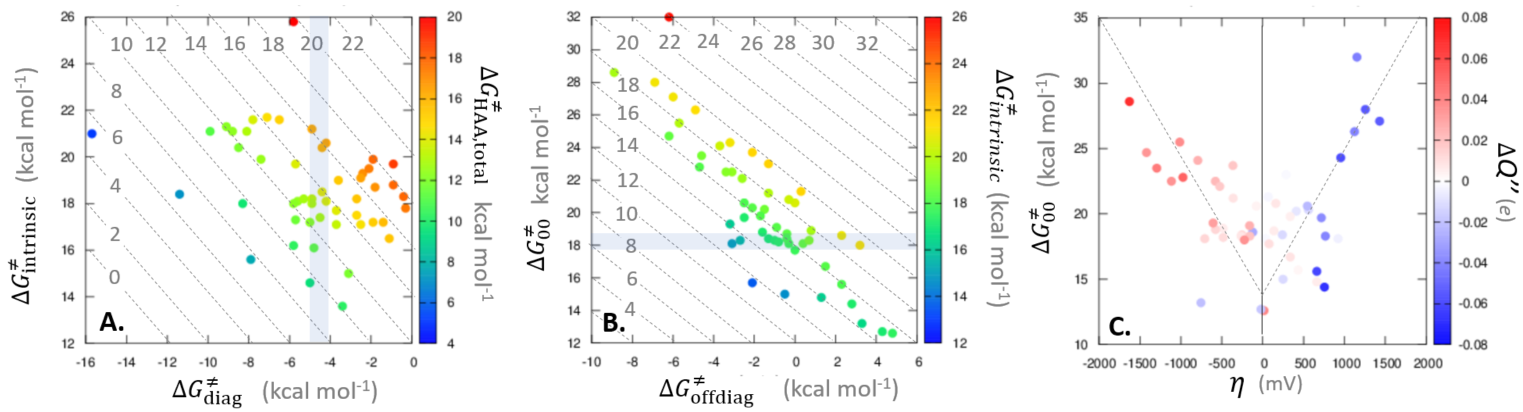

Figure S6. A. $\Delta G^{\neq}_{\mathrm{intrinsic}}$ vs. $\Delta G^{\neq}_{\mathrm{diag}}$ ($\Delta G_{0,\mathrm{inf}}/2$) and their effects on the total (tunneling-corrected) barriers $\Delta G^{\neq}_{\mathrm{HAA,total}}$ for bimolecular R-to-P HAA reactions between the C–H substrates from **Figure 2** and the 5'dAdo$^{\bullet}$ radical. The iso-contours for $\Delta G^{\neq}_{\mathrm{HAA,total}}$ are indicated. **B**. The tunneling corrected $\Delta G^{\neq}_{00}$ vs. $\Delta G^{\neq}_{\mathrm{offdiag}}$ and their effects on $\Delta G^{\neq}_{\mathrm{intrinsic}}$. The iso-contours for $\Delta G^{\neq}_{\mathrm{intrinsic}}$ are indicated. **C**. the tunneling corrected $\Delta G^{\neq}_{00}$ vs. asynchronicity η; the points are color coded according to the charge redistribution $\Delta Q''$ defined by eq 12. The analogous plots for the reactions going from reactant complexes to product complexes are given in **Figure 9**.

References:

1. Farrar, C. E., Siu, K. K., Howell, P. L., & Jarrett, J. T. (2010). Biotin synthase exhibits burst kinetics and multiple turnovers in the absence of inhibition by products and product-related biomolecules. Biochemistry, 49(46), 9985-9996.

2. Fenwick, M. K., Mehta, A. P., Zhang, Y., Abdelwahed, S. H., Begley, T. P., & Ealick, S. E. (2015). Non-canonical active site architecture of the radical SAM thiamin pyrimidine synthase. Nature communications, 6(1), 6480.

3. McLaughlin, M. I., Lanz, N. D., Goldman, P. J., Lee, K. H., Booker, S. J., & Drennan, C. L. (2016). Crystallographic snapshots of sulfur insertion by lipoyl synthase. Proceedings of the National Academy of Sciences, 113(34), 9446-9450.

4. Vey, J. L., Yang, J., Li, M., Broderick, W. E., Broderick, J. B., & Drennan, C. L. (2008). Structural basis for glycyl radical formation by pyruvate formate-lyase activating enzyme. Proceedings of the National Academy of Sciences, 105(42), 16137-16141.

5. Lepore, B. W., Ruzicka, F. J., Frey, P. A., & Ringe, D. (2005). The x-ray crystal structure of lysine-2, 3-aminomutase from Clostridium subterminale. Proceedings of the National Academy of Sciences, 102(39), 13819-13824.

6. Ruzicka, F. J., & Frey, P. A. (2007). Glutamate 2, 3-aminomutase: a new member of the radical SAM superfamily of enzymes. Biochimica et Biophysica Acta (BBA)-Proteins and Proteomics, 1774(2), 286-296.

7. Dowling, D. P., Bruender, N. A., Young, A. P., McCarty, R. M., Bandarian, V., & Drennan, C. L. (2014). Radical SAM enzyme QueE defines a new minimal core fold and metal-dependent mechanism. Nature chemical biology, 10(2), 106-112.

8. Cooper, L. E., Fedoseyenko, D., Abdelwahed, S. H., Kim, S. H., Dairi, T., & Begley, T. P. (2013). In vitro reconstitution of the radical S-adenosylmethionine enzyme MqnC involved in the biosynthesis of futalosine-derived menaquinone. Biochemistry, 52(27), 4592-4594.

9. Grell, T. A., Kincannon, W. M., Bruender, N. A., Blaesi, E. J., Krebs, C., Bandarian, V., & Drennan, C. L. (2018). Structural and spectroscopic analyses of the sporulation killing factor biosynthetic enzyme SkfB, a bacterial AdoMet radical sactisynthase. Journal of Biological Chemistry, 293(45), 17349-17361.

10. Nicolet, Y., Zeppieri, L., Amara, P., & Fontecilla-Camps, J. C. (2014). Crystal structure of tryptophan lyase (NosL): evidence for radical formation at the amino group of tryptophan. Angewandte Chemie International Edition, 53(44), 11840-11844.
11. Ding, W., Ji, X., Li, Y., & Zhang, Q. (2016). Catalytic promiscuity of the radical S-adenosyl-L-methionine enzyme NosL. Frontiers in Chemistry, 4, 27.
12. Benjdia, A., Leprince, J., Sandstrom, C., Vaudry, H., & Berteau, O. (2009). Mechanistic investigations of anaerobic sulfatase-maturating enzyme: direct Cβ H-atom abstraction catalyzed by a radical AdoMet enzyme. Journal of the American Chemical Society, 131(24), 8348-8349.
13. Feng, J., Wu, J., Dai, N., Lin, S., Xu, H. H., Deng, Z., & He, X. (2013). Discovery and characterization of BlsE, a radical S-adenosyl-L-methionine decarboxylase involved in the blasticidin S biosynthetic pathway. PloS one, 8(7), e68545.
14. Landgraf, B. J., Arcinas, A. J., Lee, K. H., & Booker, S. J. (2013). Identification of an intermediate methyl carrier in the radical S-adenosylmethionine methylthiotransferases RimO and MiaB. Journal of the American Chemical Society, 135(41), 15404-15416.
15. Hover, B. M., Loksztejn, A., Ribeiro, A. A., & Yokoyama, K. (2013). Identification of a cyclic nucleotide as a cryptic intermediate in molybdenum cofactor biosynthesis. Journal of the American Chemical Society, 135(18), 7019-7032.
16. Kim, H. J., McCarty, R. M., Ogasawara, Y., Liu, Y. N., Mansoorabadi, S. O., LeVieux, J., & Liu, H. W. (2013). GenK-catalyzed C-6′ methylation in the biosynthesis of gentamicin: isolation and characterization of a cobalamin-dependent radical SAM enzyme. Journal of the American Chemical Society, 135(22), 8093-8096.
17. Szu, P. H., Ruszczycky, M. W., Choi, S. H., Yan, F., & Liu, H. W. (2009). Characterization and mechanistic studies of DesII: a radical S-adenosyl-L-methionine enzyme involved in the biosynthesis of TDP-D-desosamine. Journal of the American Chemical Society, 131(39), 14030-14042.
18. Bridwell-Rabb, J., Zhong, A., Sun, H. G., Drennan, C. L., & Liu, H. W. (2017). A B12-dependent radical SAM enzyme involved in oxetanocin A biosynthesis. Nature, 544(7650), 322-326.

19. Grove, T. L., Radle, M. I., Krebs, C., & Booker, S. J. (2011). Cfr and RlmN contain a single [4Fe-4S] cluster, which directs two distinct reactivities for S-adenosylmethionine: methyl transfer by SN2 displacement and radical generation. Journal of the American Chemical Society, 133(49), 19586-19589.
20. Sjekloća, L., & Ferré-D'Amaré, A. R. (2022). Biochemical and structural characterization of the flavodoxin-like domain of the Schizosaccharomyces japonicus putative tRNA Phe 4-demethylwyosine synthase Tyw1 in complex with FMN. microPublication Biology, 2022.
21. Sato, S., Kudo, F., Kuzuyama, T., Hammerschmidt, F., & Eguchi, T. (2018). C-methylation catalyzed by Fom3, a cobalamin-dependent radical S-adenosyl-l-methionine enzyme in fosfomycin biosynthesis, proceeds with inversion of configuration. Biochemistry, 57(33), 4963-4966.
22. Bruender, N. A., & Bandarian, V. (2016). The radical S-adenosyl-L-methionine enzyme MftC catalyzes an oxidative decarboxylation of the C-terminus of the MftA peptide. Biochemistry, 55(20), 2813-2816.
23. Barr, I., Stich, T.A., Gizzi, A.S., Grove, T.L., Bonanno, J.B., Latham, J.A., Chung, T., Wilmot, C.M., Britt, R.D., Almo, S.C. and Klinman, J.P., 2018. X-ray and EPR characterization of the auxiliary Fe–S clusters in the radical SAM enzyme PqqE. Biochemistry, 57(8), pp.1306-1315.
24. Parent, A., Benjdia, A., Guillot, A., Kubiak, X., Balty, C., Lefranc, B., Leprince, J. and Berteau, O., 2018. Mechanistic investigations of PoyD, a radical S-adenosyl-l-methionine enzyme catalyzing iterative and directional epimerizations in polytheonamide A biosynthesis. Journal of the American Chemical Society, 140(7), pp.2469-2477.
25. Liu, W.Q., Amara, P., Mouesca, J.M., Ji, X., Renoux, O., Martin, L., Zhang, C., Zhang, Q. and Nicolet, Y., 2018. 1, 2-Diol dehydration by the radical SAM enzyme AprD4: a matter of proton circulation and substrate flexibility. Journal of the American Chemical Society, 140(4), pp.1365-1371.
26. Ding, W., Li, Y., Zhao, J., Ji, X., Mo, T., Qianzhu, H., Tu, T., Deng, Z., Yu, Y., Chen, F. and Zhang, Q., 2017. The catalytic mechanism of the class c radical S-adenosylmethionine methyltransferase NosN. Angewandte Chemie, 129(14), pp.3915-3919.

27. Benjdia, A., Guillot, A., Lefranc, B., Vaudry, H., Leprince, J. and Berteau, O., 2016. Thioether bond formation by SPASM domain radical SAM enzymes: C α H-atom abstraction in subtilosin A biosynthesis. Chemical Communications, 52(37), pp.6249-6252.